Skin Pharmacology and Physiology

Research Article

Skin Pharmacol Physiol 2023;36:27–37
DOI: 10.1159/000528403

Received: March 16, 2021
Accepted: November 24, 2022
Published online: January 24, 2023

Microinjury-Induced Tumor Necrosis Factor-α Surge Stimulates Hair Regeneration in Mice

Guang-Ri Jin[a] Su Bin Hwang[a] Hyeon Ju Park[a] Bog-Hieu Lee[a]
William A. Boisvert[b]

[a]Department of Food and Nutrition, Chung-Ang University, Anseong, Republic of Korea; [b]John A Burns School of Medicine, University of Hawaii, Honolulu, HI, USA

Keywords
Hair regeneration · Tumor necrosis factor-α · Follicular injury · Wnt signaling pathway · Vascular endothelial growth factor

Abstract
Introduction: Tumor necrosis factor (TNF)-α released after follicular injury such as that caused by plucking plays a role in the activation of hair regeneration. Microneedle (MN) treatment is applied to the scalp to increase permeability and facilitate the delivery of any number of compounds. Because the MN treatment causes injury to the epidermis, albeit minor, we reasoned that this treatment would lead to a temporary TNF-α surge and thereby promote hair regeneration. ***Methods:*** To investigate the effects of MN-treatment-induced microinjury and TNF-α on hair growth, we used C57BL/6N mice which were divided into six experimental groups: three groups of 1) negative control (NC), 2) plucking positive control (PK), and 3) MN therapy system (MTS) mice; and three groups identical to above were treated with a TNF-α blocker for 3 weeks: 4) NCB, 5) PKB, and 6) MTSB group. ***Results:*** After injury, TNF-α surge occurred on day 3 in the PK group and on day 6 in the MTS group. Wnt proteins and VEGF expression were markedly increased in the PK group on day 3 and on day 6 in the MTS group compared to the NC group. Following wound healing, only MTS and PK groups displayed thickened epidermis and longer HF length. Within the 2 weeks following treatment, the rate of hair growth was much slower in the injured mice treated with the TNF-α blocker. ***Conclusion:*** Our findings indicate that microinjury stimulates the wound-healing mechanism via TNF-α/Wnt/VEGF surge to induce hair growth, and that blocking TNF-α inhibits this growth process.

Introduction

Microneedle (MN) therapy is a method in which microchannels are created in the epidermis across the stratum corneum to increase the skin permeability in order to facilitate the absorption of small molecule drugs, proteins, and vaccines [1]. As MN-based drug delivery bypasses degradation via the digestive and hepatic system, the effects are more reproducible and consistent than delivery via oral routes [2]. In addition to drug delivery, MN therapy induces wound healing by causing microinjury to the skin [3], thereby targeting the corneocytes and keratinocyte stem cells that reside in the hair follicle (HF) [4]. HF is essential not only to hair regeneration, but also to

Karger@karger.com
www.karger.com/spp

Correspondence to:
Bog-Hieu Lee, lbheelb@cau.ac.kr
William Andrew Boisvert, wab@hawaii.edu

wound healing and skin regeneration [5]. When injury to the skin is provoked by MN, it triggers a proliferative response from adjacent cells in the epidermis and the HF. Even when superficial wounds result in removal of the surface epidermis, as long as the HFs are intact the entire wound area becomes re-epithelialized with patches of new epidermis seen spreading outward from the HFs [5]. In contrast, more profound wounds in which the HFs are damaged are slower to heal and do so only from the margins [6]. These observations strongly suggest that there is a link between HF regeneration and wound healing.

HF regeneration is defined as the process of re-entry of the HF into the anagen phase, during which multiple signal transduction pathways are activated [7]. As a cytokine that triggers the immune response, tumor necrosis factor (TNF)-α surge has been known to cause the inflammatory cascades that occur in rheumatoid arthritis or Crohn's disease [8]. According to previous in vitro studies, TNF-α has a central role in the induction of HF apoptosis [9], with some investigators reporting that HF apoptosis is a more critical factor in hair loss than dihydrotestosterone [10]. The importance of TNF-α in hair regeneration can also be deduced from a recent study in which the researchers found that hair regeneration, after plucking hair from the back skin of mice, occurred in the injured area as well as the surrounding areas through quorum-sensing behavior of macrophages. According to the report, TNF-α levels peaked 1–2 days after plucking, which was the point of HF anagen entry, and then decreased [11].

Although previous studies have examined the effectiveness of MN drug delivery in patients with alopecia [12–14], no specific mechanisms underlying the therapeutic effects of MN on wound-induced hair growth were offered. As an important component of hair regeneration, Wnt proteins are expressed in HF, which are composed of dermal papilla cells and epithelial cells, as a component of the canonical Wnt signaling pathway [15]. Together with the co-receptor lipoprotein receptor-related protein and G-protein coupled receptor, frizzled, Wnt signaling pathway allows β-catenin to translocate to the nucleus and, along with other transcription factors, facilitates the transcription of genes that regulate HF stimulation and eventual hair growth [15, 16].

The impetus for this study was in our prediction that micro-wounding by roller stimulation could induce an increase in TNF-α level and hair growth. From this, we hypothesized that the TNF-α surge is necessary for hair regrowth to occur. Thus, to investigate the therapeutic effects and mechanistic insight into MN therapy, we utilized a mouse model in which microinjury was induced in the back skin of mice by roller stimulation. After confirming increase in TNF-α production, we studied the effects of TNF-α surge and the mechanism of hair regrowth during the healing process following micro-wound induction.

Materials and Methods

Animal Experiment

The animal experiments were reviewed and approved by the Institutional Animal Care and Use Committee (IACUC) of Chung-Ang University (ID:201800026). The animals were 6-week-old male C57BL/6N mice purchased from Daehan Biolink, Inc. (Chungbuk, Korea), and maintained under controlled conditions (temperature, 23°C ± 3°C; relative humidity, 50% ± 10%; and a 12-h light/dark cycle) with ad libitum access to food and water. After a 7-day acclimatization period, experiments were performed during the following 3 weeks. All animal care and experimental procedures were performed in accordance with the Guide for the Care and Use of Laboratory Animals (8th edition, the National Academies Press, Washington, DC, USA).

The animals were divided into six groups of five mice each with 3 groups receiving and 3 not receiving the TNF-α blocker treatment. The 3 not receiving the treatment were designated as negative control (NC) group, positive plucking control (PK) group, and MN therapy system (MTS) group. The other 3 that were administered the TNF-α blocker for 3 weeks were designated as NC + TNF-α blocker (NCB) group, positive plucking control blocker + TNF-α blocker (PKB) group, and MTS + TNF-α blocker (MTSB) group (Fig. 1). Prior to the experiment, we used wax strips to remove the hair from the back skin of all mice at the same time to synchronize the HF cycle to the same refractory telogen phase.

At the end of each time period, mice were euthanized using CO_2 on experimental days 0, 3, 6, 9, 12, and 21, and samples of the back skin were collected. The collected samples were either stored at −80°C for RNA and protein extraction or fixed in 10% formalin (Sigma-Aldrich, Louis, USA).

MN Stimulation

The MN roller is made of hundreds of tiny needles which are mounted on the roller head to cause microinjury to the skin. The disk MN rollers were supplied by CNK BEAUTY Co. Ltd. (Seoul, Korea). MN stimulation was performed by applying identical strength in the same direction in the middle of the back skin of all mice by the same operator [18]. One cycle was defined as rolling the MN from the caudal to cranial skin and back to the caudal skin. After stimulation, the skin displayed mild erythema, but without swelling or bleeding. In accordance with the previous finding [17], we performed 10 cycles of rolling with a 0.5-mm MN every day for 3 weeks.

Plucking Treatment

For the PK group, we drew three 5-mm diameter circles (19.6 mm^2) on the back of each mouse by using a marker pen and plucked approximately 200 hairs evenly from the marked areas under a microscope at a density of 10 hairs/mm^2 under anesthesia [11]. With this level of injury, HF cells display TNF-α immunoreactivity and undergo regeneration through quorum-sensing signaling [11].

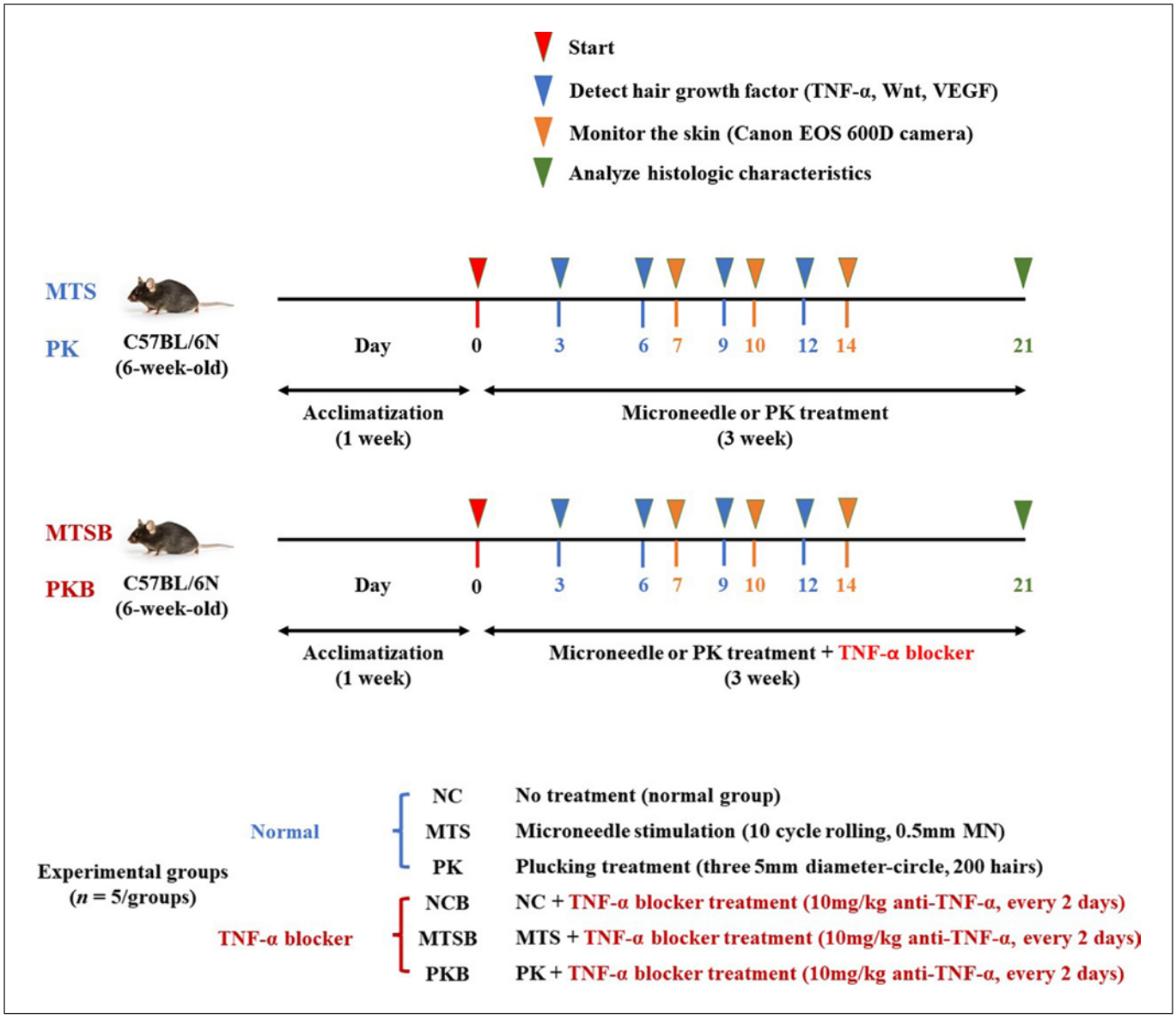

Fig. 1. A schematic describing the study design. NC, negative control; MTS, microneedle therapy system; PK, plucking; NCB, negative control blocker; MTSB, microneedle therapy system blocker; PKB, plucking blocker.

TNF-α Blocking Treatment

The NCB, MTSB, and PKB groups received the identical treatment as described above, except that a TNF-α blocker was administered. The TNF-α blocker treatment used was from an earlier publication [18]. Briefly, mice were administered intraperitoneal injections of 10 mg/kg anti-TNF-α antibody (Bio X Cell, Lebanon, USA) every two days until the end of the experiment.

Visible Comparison of Hair Growth and Skin Tissue Sampling

The day the treatment was administered the first time was defined as day 1. Thereafter, the mice were monitored daily, and the measurements related to hair growth were made on days 1, 7, 10, and 14.

Real-Time PCR

To determine the extent of TNF-α signaling involved in hair growth, the relative mRNA expression of four molecules (TNF-α, Wnt3, Wnt10a, and Wnt10b) was quantified. Total RNA was extracted by using RNeasy Fibrous Tissue Mini Kit (Qiagen, Dusseldorf, Germany) in accordance with the manufacturer's instructions. cDNA was synthesized from 1 μg of total RNA by using RevertAid First Strand cDNA Synthesis Kit (Thermo Fisher Scientific Inc, Waltham, USA). PCR was performed using a Piko Real™ 96 real-time PCR system (Thermo Fisher Scientific Inc, Waltham, USA) using Maxima SYBR Green/ROX qPCR Master Mix and the following reaction parameter: pre-denaturation at 95°C for 10 min, followed by 40 cycles of 95°C for 15 s,

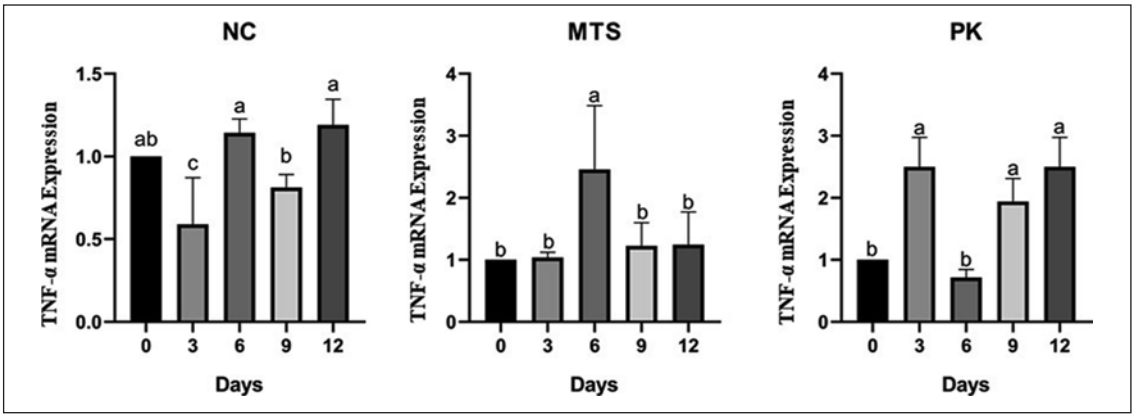

Fig. 2. TNF-α mRNA expression in the mouse dorsal skin following different treatments. All experiments were performed in triplicate. Values are mean ± standard deviation, and values with different superscript letters differ significantly at $p < 0.05$ by Duncan's multiple range test. NC, negative control; MTS, microneedle therapy system; PK, plucking.

60°C for 30 s, and 72°C for 30 s. The primer sets were purchased from Bioneer (Daejeon, Korea). The primer sequences for each gene, including GAPDH used as the housekeeping gene, are shown in online supplementary Table 1 (for all online suppl. material, see www.karger.com/doi/10.1159/000528403).

Western Blotting

Protein was extracted from the mouse back skin by incubation in RIPA buffer and protease inhibitor (Thermo Fisher Scientific Inc, Waltham, USA) and quantified using a bicinchoninic acid assay. 30 μg of protein was run on 10% sodium dodecyl sulfate-polyacrylamide gel electrophoresis and transferred to polyvinylidene fluoride membranes (Millipore, Billerica, USA). Nonspecific binding to the membrane was blocked for 1 h at room temperature using 5% BSA solution in Tris-buffered saline Tween-20 (20-mm Tris, pH 7.6; 136-mm NaCl; 0.1% Tween-20). The primary antibodies to TNF-α (Cell Signaling Technology, Danvers, USA) and VEGF (Santa Cruz Biotechnology Inc, Dallas, USA) were diluted at 1:1,000, incubated overnight at 4°C, and then incubated with HRP-conjugated goat anti-rabbit IgG (Santa Cruz Biotechnology Inc, Dallas, USA) at a dilution of 1:1,000 for 1 h at RT. Subsequently, protein expression was measured by using enhanced chemiluminescence system (Thermo Fisher Scientific Inc, Waltham, USA).

Histological Assessment of Back Skin and Visual Inspection of Hair Growth

H&E staining on the back skin samples was performed using the routine Mayer method [19]. After formalin fixation, samples were processed using an ascending series of graded ethanol and cleared in xylene (Sigma-Aldrich, Louis, USA). Subsequently, each tissue piece was resected, placed in a cassette to be incubated with paraffin for 24 h in Tissue-Tek® Auto TEC® automated embedder (Sakura, San Francisco, USA), and then mounted into a paraffin block. Using a microtome (Leica, Wetzlar, Germany), 4-μm-thick sections were cut from each paraffin-embedded tissue and affixed to a glass slide. Each slide was stained with H&E (Sigma-Aldrich, Louis, USA) with a slide stainer (Shandon Linistain GLX, Shandon Inc., Pittsburgh, USA). The shape of the follicles from each stained section was viewed by an experienced veterinary pathologist using a light microscope (Leica, Wetzlar, Germany) at ×100 magnification, and the skin thickness and follicle depth were measured using the scale bar of the microscope program. The hair growth-related characteristics on the treated skin were measured on days 1, 7, 10, and 14 using photographs taken with a Canon EOS 600D camera (Canon Corp, Tokyo, Japan).

Statistics

The data were analyzed by using SPSS Statistics ver 23.0 (SPSS Inc., Chicago, USA). For between-group statistical analyses, a one-way ANOVA and Duncan's multiple range test were performed. A between-group difference was considered statistically significant if the p value <0.05. Student's t test was also used to analyze the data with statistical significance defined as $^{*}p < 0.05$, $^{**}p < 0.01$, and $^{***}p < 0.001$. All experiments were repeated three times to assess reproducibility. All data are expressed as the mean ± standard deviation.

Results

TNF-α mRNA Expression in Mouse Back Skin by Treatment Type

We measured the changes in TNF-α mRNA expression in the back skin based on the type of injury (Fig. 2). In the NC group, TNF-α expression decreased on day 3 relative to day 0 ($p < 0.05$) and was not significantly changed on days 6, 9, and 12, remaining at levels similar to day 0. In the MTS group, a significant TNF-α surge occurred on day 6 compared with day 0, with levels returning to baseline values on days 9 and 12. In the PK group, there was an initial TNF-α surge on day 3, which returned to the basal level on day 6 and then surged again on days 9 and 12 (Fig. 2). In contrast, none of the groups treated with TNF-α blocker showed a TNF-α surge, and there was a tendency for decreased TNF-α levels (data not shown).

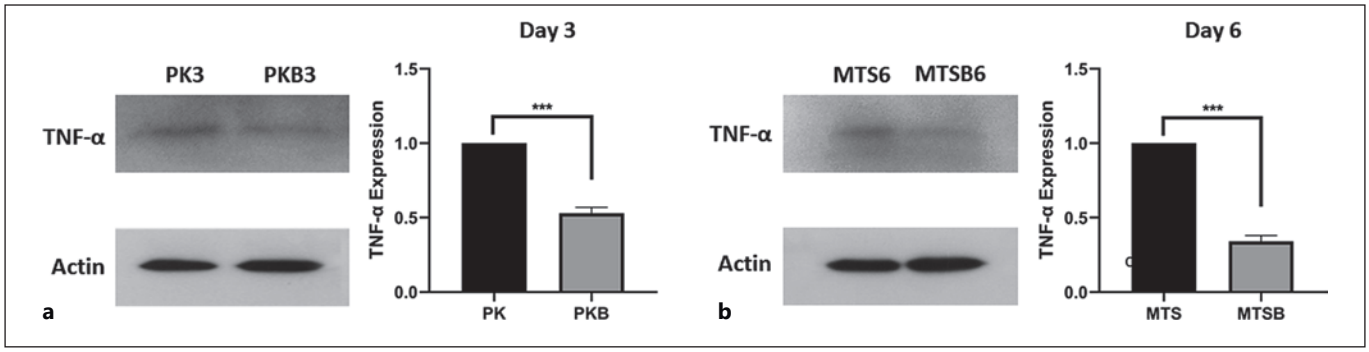

Fig. 3. Protein expression of TNF-α at the time of TNF-α surge. **a** TNF-α protein expression in PK and PKB group on day 3. **b** TNF-α protein expression in MTS and MTSB group on day 6. All experiments were performed in triplicate. Each data bar represents mean ± standard deviation. *** indicates statistical difference with $p < 0.001$ by Student's *t* test. MTS, microneedle therapy system; MTSB, microneedle therapy system blocker; PK, plucking; PKB, plucking blocker.

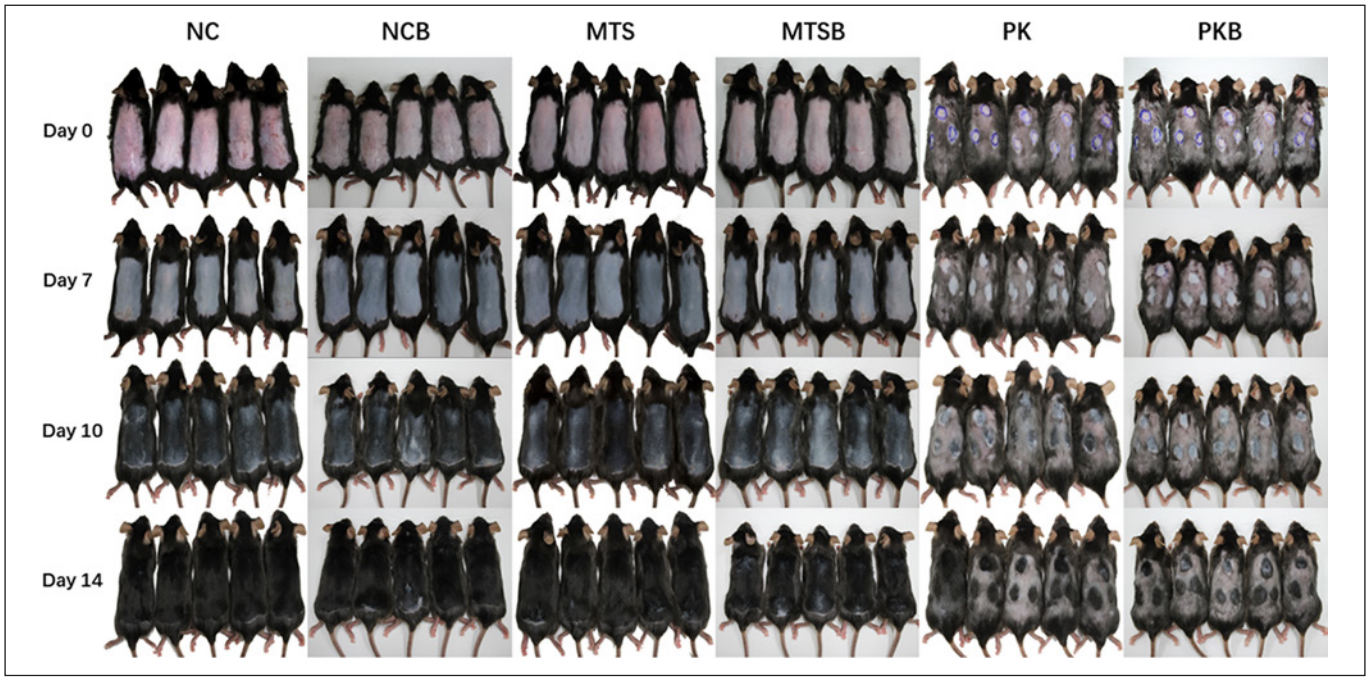

Fig. 4. Pattern of hair growth in mouse dorsal skin over the 3-week experimental period following various treatments. NC, negative control; NCB, negative control blocker; MTS, microneedle therapy system; MTSB, microneedle therapy system blocker; PK, plucking; PKB, plucking blocker.

Quantitative analysis of TNF-α expression revealed a clear surge, with a 2.5-fold increase from day 0–6 in the MTS group and 2.5-fold increase from day 0–3 in the PK group. These results show that the injury-induced TNF-α surge occurred at similar levels after HF injury regardless of whether the injury was caused by plucking or MN, suggesting that TNF-α surge can occur with relatively minor injury.

TNF-α Blockade Efficacy

To assess the inhibitory effect of the TNF-α antibody treatment on TNF-α surge, we measured the TNF-α protein expression in the mouse back skin at the time of TNF-α surge. Treatment with the TNF-α blocker led to a substantial decrease in the TNF-α protein as shown in the Western blots of the MTSB6 and PKB3 groups compared

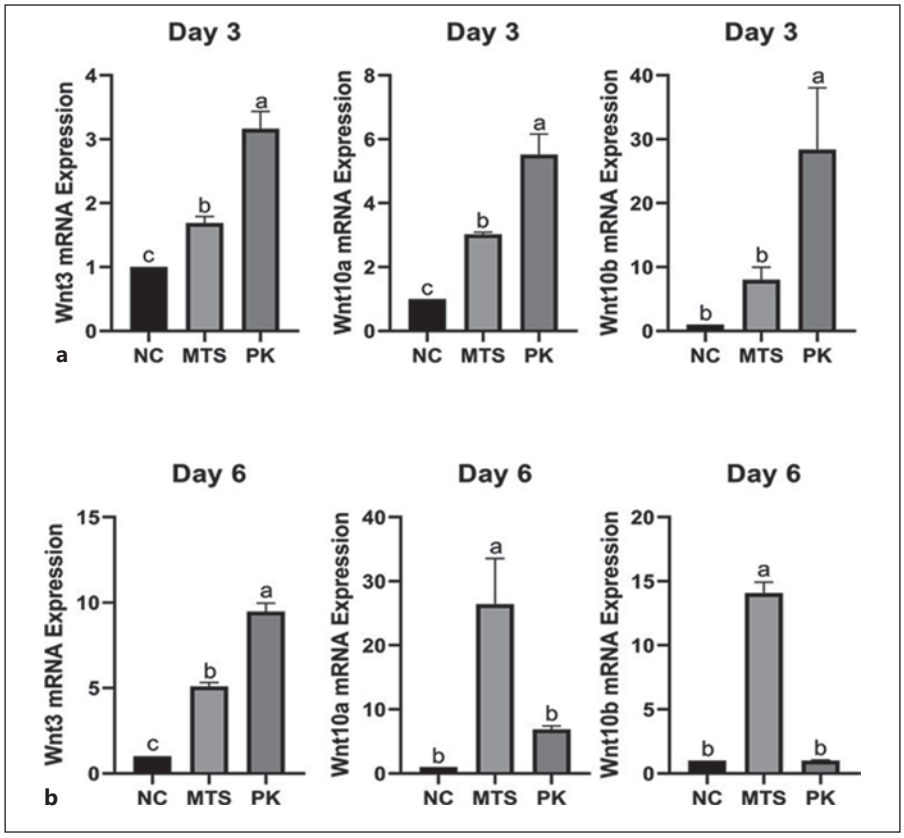

Fig. 5. Wnt mRNA expression at the time of TNF-α surge. **a** Wnt3, Wnt10a, and Wnt10b mRNA expression on day 3. **b** Wnt3, Wnt10a, and Wnt10b mRNA expression on day 6. All experiments were performed in triplicate. Values are mean ± standard deviation, and values with different superscript letters differ significantly at $p < 0.05$ by Duncan's multiple range test. NC, negative control; MTS, microneedle therapy system; PK, plucking.

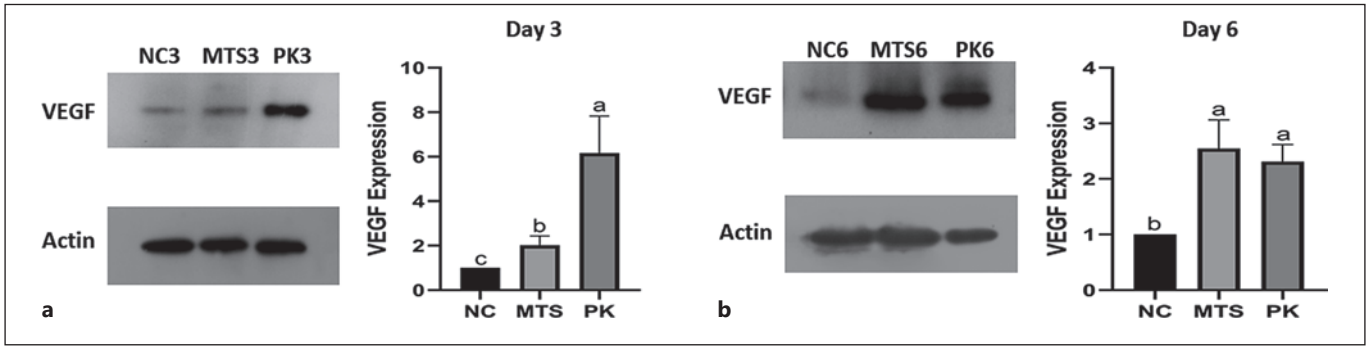

Fig. 6. Protein expression of VEGF at the time of TNF-α surge. **a** VEGF protein expression following different treatments on day 3. **b** VEGF protein expression following different treatments on day 6. All experiments were performed in triplicate. Values are mean ± standard deviation, and values with different superscript letters differ significantly at $p < 0.05$ by Duncan's multiple range test. NC, negative control; MTS, microneedle therapy system; PK, plucking.

to their counterpart with no blocker treatment (Fig. 3). The TNF-α protein expression was decreased by 65% in the MTSB group compared with MTS group on day 6, and by 54% in the PKB group compared with PK group on day 3 (Fig. 3). These results confirmed that the antibody treatment was successful in inhibiting TNF-α protein levels in the skin.

Assessment of Hair Growth Pattern

The pattern of mouse hair growth, as determined by visual inspection over the 3-week experimental period, is shown in Figure 4. From day 7, the skin color of mice in the NC and MTS group changed from apricot to dark gray, whereas in the PK group, the color of the injured site was observed to be light gray until day 7. On day 10, mice in the

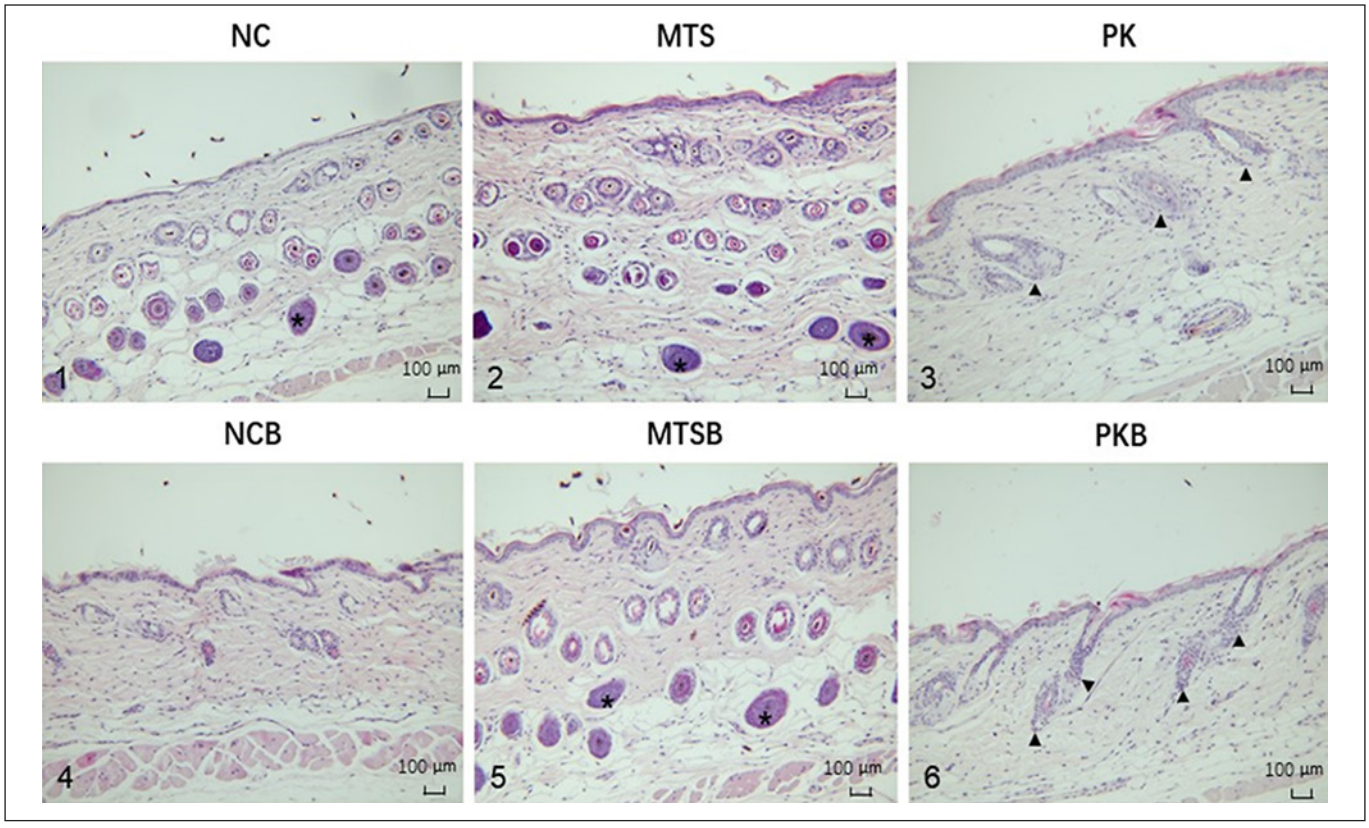

Fig. 7. Histologic characteristics of hair follicles representing different treatments of dorsal tissues on day 21. In the MTS group, an enlarged lumen was observed in the growing hair follicle (*), whereas in the PK group the cell layer surrounding HF was greatly amplified (▲). NC, negative control; NCB, negative control blocker; MTS, microneedle therapy system; MTSB, microneedle therapy system blocker; PK, plucking; PKB, plucking blocker.

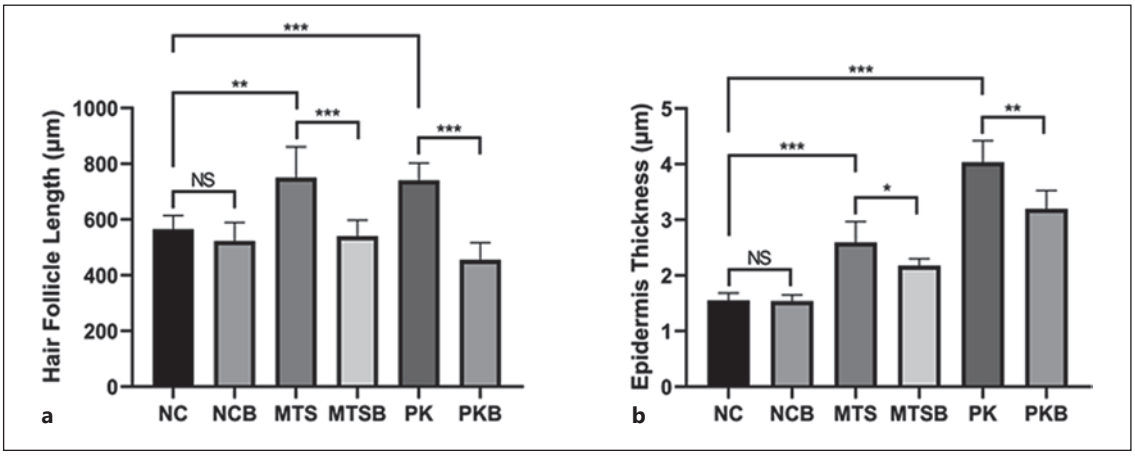

Fig. 8. Hair follicle length and epidermal thickness as a result of different dorsal tissue treatments on day 21. Comparison of hair follicle length is shown in **a**, whereas comparison of epidermal thickness is shown in **b**. All experiments were performed in triplicate. Each data bar represents mean ± standard deviation. *, **, and *** indicate statistical difference with $p < 0.05$, $p < 0.01$, and $p < 0.001$ by Student's t test, respectively. NS means not significant. NC, negative control; NCB, negative control blocker; MTS, microneedle therapy system; MTSB, microneedle therapy system blocker; PK, plucking; PKB, plucking blocker.

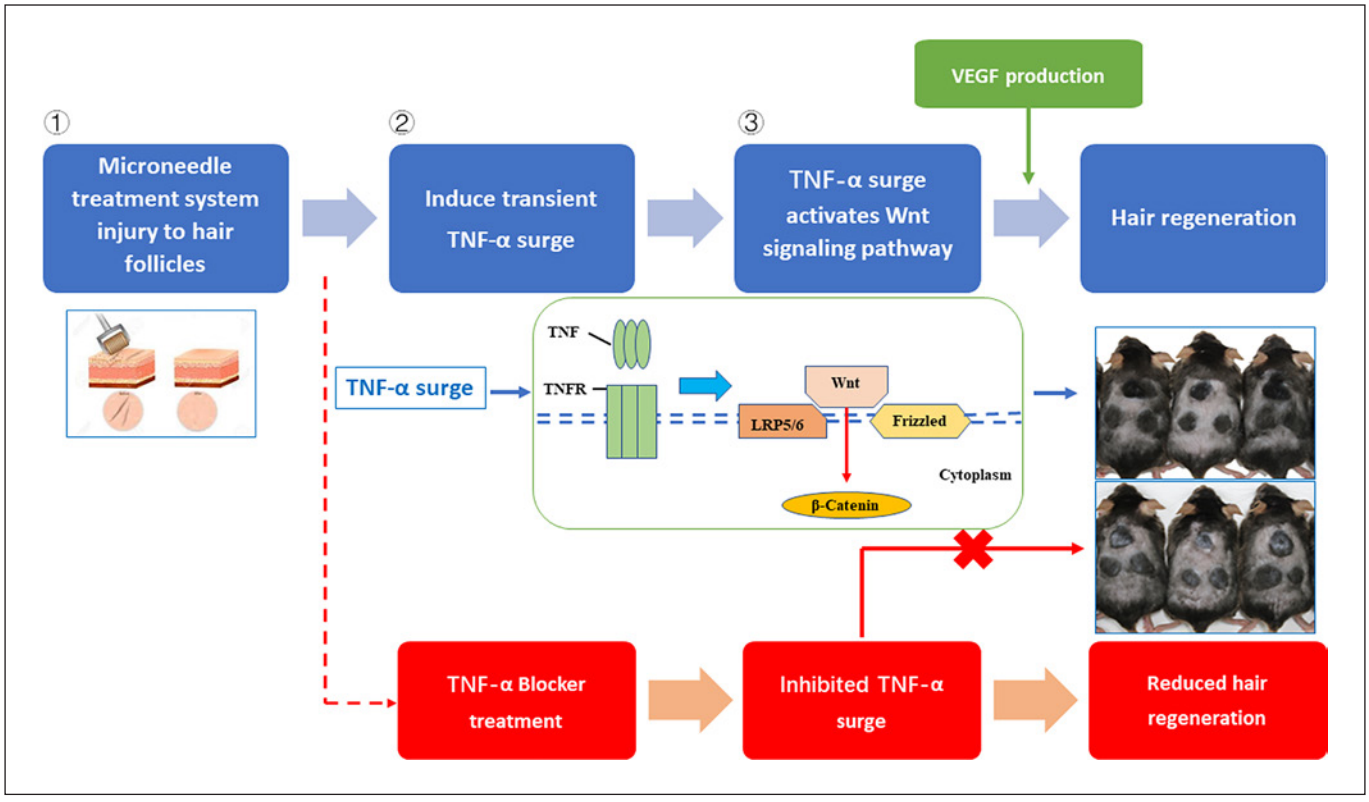

Fig. 9. Cartoon depicting the events that follow microneedle therapy injury to hair follicle. Injury to the back skin leads to TNF-α surge which in turn activates the Wnt signaling pathway that involves LRP5/6 and frizzled proteins eventually resulting in B-catenin activation that directly enhances hair regeneration. Treatment with TNF-a blocker reduces the TNF-α surge resulting in reduced hair regeneration.

NC and MTS group, but not the PK group, showed gradual hair regeneration which reached ≥90% by day 14. In the PK group, plucking within a 0.5-cm-diameter area resulted in rapid hair growth from day 10–14. In contrast, in all 3 TNF-α blocker groups (NCB, MTSB, and PKB) there was markedly slower hair growth from day 10 relative to the normal groups (NC, MTS, PK). On day 14, the MTSB mice showed patches of gray in the back skin, whereas MTS mice showed nearly full coverage. Similarly, in the PKB group the color remained gray in the 0.5-cm-diameter plucked areas as compared to fully black color shown in the patches of mice in the PK group. These results suggest that hair regeneration was delayed in the groups treated with a TNF-α blocker relative to the normal groups, confirming that the TNF-α surge is a prerequisite for a full hair regrowth.

Wnt Expression during TNF-α Surge

Because we observed TNF-α surge on day 6 in the MTS group and on day 3 in the PK group, we measured Wnt mRNA expression in the mouse back skin on days 3 and 6 for each experimental group (Fig. 5). Relative to the NC group, Wnt3 expression on day 3 was increased by 1.7-fold in the MTS group and by 3.2-fold in the PK group. Wnt10a expression was increased 3.0-fold in the MTS group and 5.5-fold in the PK group, whereas Wnt10b expression was increased 8.0-fold in the MTS group and 28.4-fold in the PK group (Fig. 5a). In addition, on day 6 relative to the NC group, Wnt3 expression was increased 5.1-fold in the MTS group and 9.5-fold in the PK group whereas Wnt10a expression was increased 26.4-fold in the MTS group and 6.9-fold in the PK group and Wnt10b expression was raised 14.1-fold in the MTS group and no change in the PK group (Fig. 5b).

VEGF Protein Expression at the Time of the TNF-α Surge

Although MTS and PK treatments result in varying types and severity of injury, both types of injuries are healed through the classic wound-healing process [17, 20]. In this process, VEGF serves as a critical factor in

promoting angiogenesis and regeneration. To determine if VEGF indeed played a role in the post-treatment healing of our MTS and PK mice, we measured VEGF protein expression in the back skin of the two groups of mice at the time of TNF-α surge (Fig. 6). On day 3, VEGF protein expression was significantly higher, relative to the NC group, by 2.0-fold in the MTS group and by 6.2-fold in the PK group (Fig. 6a). On day 6, the expression level was 2.6-fold higher in the MTS group and 2.3-fold higher in the PK group compared to the NC group (Fig. 6b). These results indicated that VEGF likely plays a role in the wound-healing process after injury caused by MTS and PK treatments.

Histologic Characteristics of HFs

H&E staining results are presented in Figure 7. In the NC group, the majority of HFs in the dermis showed normal growth at 21 days post-stripping. In the MTS group, the number of HFs observed in the dermis was increased compared with the control, whereas the hair thickness decreased. Interestingly, in the PK group, parts of keratinized epithelium and epidermis grew thicker by 2–3 layers, relative to NC. In addition, although the number of dermal HFs appeared to have decreased, lumen of the growing HF was enlarged relative to normal tissue, and the surrounding cell layer was greatly amplified. In comparison, the TNF-α blocker groups showed significantly diminished number of HFs compared with their control counterparts.

We next measured the HF length and epidermal thickness as shown in Figure 8a, b, respectively. HF length was significantly longer in the MTS (750 μm) and PK (740 μm) groups compared with the NC (565 μm) group ($p < 0.05$). Among the groups that received the TNF-α blocker, the measured lengths were 523 μm, 540 μm, and 455 μm in the NCB, MTSB, and PKB groups, respectively (Fig. 8a). Furthermore, the MTS and PK groups that exhibited TNF-α surge had significantly longer HF length than the MTSB and PKB groups.

Epidermal thickness was also significantly greater in the MTS and PK group relative to that in the NC group ($p < 0.05$), which was measured to be 1.55 μm in the NC group, 2.52 μm in the MTS group, and 4.03 μm in the PK group. Within the groups receiving the TNF-α blocker, the epidermal thickness was 1.54 μm in the NCB mice, 2.25 μm in the MTSB mice, and 3.20 μm in the PKB mice, demonstrating that the epidermis was thicker in the MTS and PK groups compared to the respective TNF-α blocker groups (Fig. 8b). Moreover, the number of corneocytes in the thickened epidermis was greater than in the thinner epidermis of the TNF-α blocker groups (Fig. 7).

Discussion

Similar to a previous study in which plucking led to an early surge in TNF-α [11], we observed an early surge in TNF-α at day 3 with plucking and on day 6 with MN stimulation. Although the surge levels were similar, the difference in timing may be due to plucking inducing more severe injury to the HFs than the microneedle method. The dependence of wound healing and hair growth on TNF-α has been demonstrated by delayed wound healing and inhibition of hair growth in TNF-α knockout mice [21]. Using an anti-TNF-α antibody, we also observed a marked inhibition of hair growth in the TNF-α blocker groups, which confirms our hypothesis that the TNF-α surge is implicated as a key element in wound-induced hair growth.

We believe that MN stimulation-mediated TNF-α surge along with concomitant increase in expression of Wnt3, Wnt10a, and Wnt10b, the signaling factors related to hair regeneration, led to hair growth in our MTS mice. Wnt signal transduction pathway is known to regulate hair growth and influence hair shaft structure [16]. Increases in Wnt3, Wnt10a, and Wnt10b promote activation of the Wnt/β-catenin signal transduction pathway, the activation of which not only initiates hair morphogenesis, but is also a critical modulator of HF regeneration and the growth of the hair shaft [22]. Mechanistically, Wnt3 and Wnt10a mediate the canonical Wnt signaling pathway which induces β-catenin stabilization [23], whereas Wnt10b promotes HF proliferation and maintains the trichogenesis-promoting ability [24].

VEGF is an important vascular growth factor that facilitates cell survival and proliferation [25]. In addition, it is known to play an integral role in angiogenesis-related inflammation and various cancers [26]. In mice with MN injury, VEGF is expressed during wound healing and causes supercompensation. We suspect that the blood vessels of the dermis in the back tissue were affected by MN stimulation to undergo vasodilation, angiogenesis, and regeneration, and that such vascular responses provided an increased nutritional supply to the HF to prolong its anagen phase. Minoxidil is an FDA-approved medication for the treatment of male-pattern hair loss, which also increases VEGF expression in hDPCs [27]. The present study demonstrated that the effects of MN stimulation may occur through a similar mechanism to minoxidil and confirm previous findings that an increase in VEGF facilitates hair growth [28, 29].

Histologic results showed that on day 21, an increase in HF length was observed in the MTS and PK groups relative to the TNF-α blocker groups, and that the cell

layer surrounding the HF was greatly amplified. HF length was determined to be mediated, at least in part, by the persistence of the anagen phase which suggests that the injury-induced TNF-α surge helps prolong and maintain the anagen phase. In mammals, epidermis is seen as a complex and dynamic tissue as there is quick cell turnover in the interfollicular epidermis and HFs undergo cyclic phases. Maintenance of the epidermis depends on a population of multipotential stem cells that have the ability to generate all of the differentiated epidermal lineages [30]. In the current study, the epidermis of the mouse dorsal skin was markedly thickened in the MTS and PK group compared with the NC, NCB, MTSB, and PKB groups. This may be due to the expression of epidermal growth factor (EGF) in the MTS and PK epidermis as a result of injury stemming from MN and PK stimulation. It has been reported that EGF in saliva accelerates wound healing in skin [31, 32] and that during healing process, mesenchymal stem cells are induced to differentiate into DPCs and promote HF regeneration [33]. It stands to reason that EGF expression after MN or PK treatment may have helped maintain the HF anagen phase. Furthermore, several Wnts and their frizzled receptors are expressed in the epidermis in a highly dynamic and complex pattern [34]. Transgenic mice in which the Wnt pathway is blocked in the epidermis have progressive hair loss [35, 36]. Furthermore, the major effect of transient activation of β-catenin in adult epidermis appears to be to promote anagen phase of the hair cycle [37].

Conclusion

In conclusion, the TNF-α surge observed in the present study caused DPCs present in HFs to promote the expression of hair growth factors such as Wnt3, Wnt10a, and Wnt10b, and to induce the transition from telogen phase to anagen phase while blocking entry to the catagen phase. Furthermore, increased VEGF expression allowed DPCs access to increased nutritional supply from the circulation to undergo active metabolism. In terms of hair growth, our study demonstrates that MN stimulation causes microinjuries in the skin which induces a TNF-α surge as a part of the wound-healing mechanism and results in measurable hair growth. The sequence of events following MN injury including TNF-α surge and the Wnt pathway and VEGF production that eventually led to hair regeneration is shown in Figure 9. The figure also demonstrates the inhibition of hair growth following treatment with TNF-α blocker. Although the positive effects that we observed seem to offer a potential hair loss treatment, to apply the findings to the treatment of alopecia additional experiments must be conducted to include the effects of other growth factors known to influence hair growth such as hepatocyte growth factor, insulin-like growth factor 1, and keratinocyte growth factor during wound healing.

Statement of Ethics

Animal experiments were approved by the Institutional Animal Care and Use Committee (IACUC) of Chung-Ang University (approval number:201800026).

Conflict of Interest Statement

The authors have no conflicts of interest to declare.

Funding Sources

This work was supported by the Basic Science Research Program through the National Research Foundation of Korea (NRF) funded by the Ministry of Education, Science and Technology (NRF-2017R1D1A1B03033507).

Author Contributions

Guang-Ri Jin performed the experiments, analyzed the data, performed literature research, and drafted the manuscript. Su Bin Hwang and Hyeon Ju Park performed the experiments. William Boisvert contributed to study conception and design as well as writing of the manuscript. Bog-Hieu Lee contributed to study conception and design, analyzed the data, and drafted the manuscript.

Data Availability Statement

All data generated or analyzed during this study are included in this article and its supplementary material files. Further inquiries can be directed to the corresponding authors.

References

1 Henry S, McAllister DV, Allen MG, Prausnitz MR. Microfabricated microneedles: a novel approach to transdermal drug delivery. J Pharm Sci. 1998;87(8):922–5.
2 Prausnitz MR. Microneedles for transdermal drug delivery. Adv Drug Deliv Rev. 2004;56(5):581–7.
3 McCrudden MT, McAlister E, Courtenay AJ, Gonzalez-Vazquez P, Singh TR, Donnelly RF. Microneedle applications in improving skin appearance. Exp Dermatol. 2015;24(8):561–6.

4 Ansell DM, Kloepper JE, Thomason HA, Paus R, Hardman MJ. Exploring the "hair growth-wound healing connection": anagen phase promotes wound re-epithelialization. J Invest Dermatol. 2011;131(2):518–28.
5 Ito M, Cotsarelis G. Is the hair follicle necessary for normal wound healing? J Invest Dermatol. 2008;128(5):1059–61.
6 Bishop GH. Regeneration after experimental removal of skin in man. Am J Anat. 1945;76(2):153–81.
7 Schneider MR, Schmidt-Ullrich R, Paus R. The hair follicle as a dynamic miniorgan. Curr Biol. 2009;19(3):R132–142.
8 Locksley RM, Killeen N, Lenardo MJ. The TNF and TNF receptor superfamilies: integrating mammalian biology. Cell. 2001;104(4):487–501.
9 Botchkareva NV, Ahluwalia G, Shander D. Apoptosis in the hair follicle. J Invest Dermatol. 2006;126(2):258–64.
10 Mikkola ML. TNF superfamily in skin appendage development. Cytokine Growth Factor Rev. 2008;19(3–4):219–30.
11 Chen CC, Wang L, Plikus MV, Jiang TX, Murray PJ, Ramos R, et al. Organ-level quorum sensing directs regeneration in hair stem cell populations. Cell. 2015;161(2):277–90.
12 Yang G, Chen Q, Wen D, Chen Z, Wang J, Chen G, et al. A therapeutic microneedle patch made from hair-derived keratin for promoting hair regrowth. ACS Nano. 2019;13(4):4354–60.
13 Lee JS, Hwang Y, Oh H, Kim S, Kim JH, Lee JH, et al. A novel chitosan nanocapsule for enhanced skin penetration of cyclosporin A and effective hair growth in vivo. Nano Res. 2019;12:3024–30.
14 Fakhraei Lahiji S, Seo SH, Kim S, Dangol M, Shim J, Li CG, et al. Transcutaneous implantation of valproic acid-encapsulated dissolving microneedles induces hair regrowth. Biomaterials. 2018;167:69–79.
15 Ouji Y, Ishizaka S, Yoshikawa M. Dermal papilla cells serially cultured with Wnt-10b sustain their hair follicle induction activity after transplantation into nude mice. Cell Transpl. 2012;21(10):2313–24.
16 Millar SE, Willert K, Salinas PC, Roelink H, Nusse R, Sussman DJ, et al. WNT signaling in the control of hair growth and structure. Dev Biol. 1999;207(1):133–49.
17 Kim YS, Jeong KH, Kim JE, Woo YJ, Kim BJ, Kang H. Repeated microneedle stimulation Induces enhanced hair growth in a murine model. Ann Dermatol. 2016;28(5):586–92.
18 Grinberg-Bleyer Y, Dainichi T, Oh H, Heise N, Klein U, Schmid RM, et al. Cutting edge: NF-κB p65 and c-Rel control epidermal development and immune homeostasis in the skin. J Immunol. 2015;194(6):2472–6.
19 Garvey W. Modification of the mayer hematoxylin stain. J Histotechnology. 2013;14(3):163–5.
20 Park JH, Choi SO, Seo S, Choy YB, Prausnitz MR. A microneedle roller for transdermal drug delivery. Eur J Pharm Biopharm. 2010;76(2):282–9.
21 Lei M, Guo H, Qiu W, Lai X, Yang T, Widelitz RB, et al. Modulating hair follicle size with Wnt10b/DKK1 during hair regeneration. Exp Dermatol. 2014;23(6):407–13.
22 Myung PS, Takeo M, Ito M, Atit RP. Epithelial Wnt ligand secretion is required for adult hair follicle growth and regeneration. J Invest Dermatol. 2013;133(1):31–41.
23 Guo H, Xing Y, Liu Y, Luo Y, Deng F, Yang T, et al. Wnt/beta-catenin signaling pathway activates melanocyte stem cells *in vitro* and *in vivo*. J Dermatol Sci. 2016;83(1):45–51.
24 Wang X, Chen H, Tian R, Zhang Y, Drutskaya MS, Wang C, et al. Macrophages induce AKT/β-catenin-dependent Lgr5+ stem cell activation and hair follicle regeneration through TNF. Nat Commun. 2017;8:14091.
25 Zachary I, Gliki G. Signaling transduction mechanisms mediating biological actions of the vascular endothelial growth factor family. Cardiovasc Res. 2001;49(3):568–81.
26 Ferrara N, Davis-Smyth T. The biology of vascular endothelial growth factor. Endocr Rev. 1997;18(1):4–25.
27 Lachgar S, Charveron M, Gall Y, Bonafe JL. Minoxidil upregulates the expression of vascular endothelial growth factor in human hair dermal papilla cells. Br J Dermatol. 1998;138(3):407–11.
28 Rho SS, Park SJ, Hwang SL, Lee MH, Kim CD, Lee IH, et al. The hair growth promoting effect of *Asiasari radix* extract and its molecular regulation. J Dermatol Sci. 2005;38(2):89–97.
29 Li M, Marubayashi A, Nakaya Y, Fukui K, Arase S. Minoxidil-induced hair growth is mediated by adenosine in cultured dermal papilla cells: possible involvement of sulfonylurea receptor 2B as a target of minoxidil. J Invest Dermatol. 2001;117(6):1594–600.
30 Niemann C, Watt FM. Designer skin: lineage commitment in postnatal epidermis. Trends Cell Biol. 2002;12(4):185–92.
31 Jahovic N, Guzel E, Arbak S, Yeğen BC. The healing-promoting effect of saliva on skin burn is mediated by epidermal growth factor (EGF): role of the neutrophils. Burns. 2004;30(6):531–8.
32 Noguchi S, Ohba Y, Oka T. Effect of salivary epidermal growth factor on wound healing of tongue in mice. Am J Physiol. 1991;260(4 Pt 1):E620–5.
33 Bai T, Liu F, Zou F, Zhao G, Jiang Y, Liu L, et al. Epidermal growth factor induces proliferation of hair follicle-derived mesenchymal stem cells through epidermal growth factor receptor-mediated activation of ERK and AKT signaling pathways associated with upregulation of cyclin D1 and downregulation of p16. Stem Cell Dev. 2017;26(2):113–22.
34 Reddy S, Andl T, Bagasra A, Lu MM, Epstein DJ, Morrisey EE, et al. Characterization of Wnt gene expression in developing and postnatal hair follicles and identification of Wnt5a as a target of Sonic hedgehog in hair follicle morphogenesis. Mech Dev. 2001;107(1–2):69–82.
35 Merrill BJ, Gat U, DasGupta R, Fuchs E. Tcf3 and Lef1 regulate lineage differentiation of multipotent stem cells in skin. Genes Dev. 2001;15(13):1688–705.
36 Niemann C, Owens DM, Hülsken J, Birchmeier W, Watt FM. Expression of ΔNLef1 in mouse epidermis results in differentiation of hair follicles into squamous epidermal cysts and formation of skin tumours. Development. 2002;129(1):95–109.
37 Van Mater D, Kolligs FT, Dlugosz AA, Fearon ER. Transient activation of β-catenin signaling in cutaneous keratinocytes is sufficient to trigger the active growth phase of the hair cycle in mice. Genes Dev. 2003;17(10):1219–24.